

Astrocytes Are the Primary Source of Tissue Factor in the Murine Central Nervous System

A Role for Astrocytes in Cerebral Hemostasis

Michael Eddleston,* Juan Carlos de la Torre,* Michael B. A. Oldstone,*
David J. Loskutoff,† Thomas S. Edgington,‡ and Nigel Mackman‡

*Division of Virology, Department of Neuropharmacology, †Committee on Vascular Biology, and

‡Department of Immunology, The Scripps Research Institute, La Jolla, California 92037

Abstract

Hemostasis in the brain is of paramount importance because bleeding into the neural parenchyma can result in paralysis, coma, and death. Consistent with this sensitivity to hemorrhage, the brain contains large amounts of tissue factor (TF), the major cellular initiator of the coagulation protease cascades. However, to date, the cellular source for TF in the central nervous system has not been identified. In this study, analysis of murine brain sections by *in situ* hybridization demonstrated high levels of TF mRNA in cells that expressed glial fibrillary acidic protein, a specific marker for astrocytes. Furthermore, primary mouse astrocyte cultures and astrocyte cell lines from mouse, rat, and human constitutively expressed TF mRNA and functional protein. These data indicated that astrocytes are the primary source of TF in the central nervous system. We propose that astrocytes forming the glia limitans around the neural vasculature and deep to the meninges are intimately involved in controlling hemorrhage in the brain. Finally, we observed an increase in TF mRNA expression in the brains of scrapie-infected mice. This modulation of TF expression in the absence of hemorrhage suggested that TF may function in processes other than hemostasis by altering protease generation in normal and diseased brain. (*J. Clin. Invest.* 1993. 92:349–358.) **Key words:** blood coagulation · hemorrhage · stroke · neural vasculature · scrapie infection

Introduction

The brain must use efficient mechanisms to limit hemorrhage in the central nervous system (CNS)¹. Intracranial hemor-

rhage, whether resulting from cerebrovascular disease or acute brain trauma, can result in paralysis, coma, and death. Stroke is currently the third leading cause of death and the primary cause of disabilities in the Western hemisphere (1, 2). Fibrinolysis of the occluding thrombus after a stroke leads to reperfusion of damaged hypoxic vessels and diffuse petechial bleeding into the parenchyma from the damaged microvasculature (reviewed in reference 3). This bleeding is often toxic to neuronal function, radically altering the unique neural microenvironment formed by the blood-brain barrier.

Tissue factor (TF), also known as tissue thromboplastin, is the primary cellular initiator of the coagulation protease cascades (reviewed in references 4–6). Activation of these cascades results in the generation of thrombin, a pleiotropic agonist for cells bearing the thrombin receptor (reviewed in reference 7), and ultimately in the deposition of fibrin. TF is a member of the cytokine/hematopoietic growth factor receptor family (8) and is constitutively expressed by extravascular cells, such as cells in the tunica adventitia surrounding major vessels and cells delimiting organ boundaries (9, 10). When vascular integrity is disrupted, binding of plasma Factor VII/VIIa to TF expressed on extravascular cells initiates the coagulation protease cascades by activating both Factors IX and X. Thus, TF plays a pivotal role in initiating blood coagulation. Consistent with this role for TF in hemostasis and the great sensitivity of the brain to hemorrhage, high levels of TF mRNA and functional protein are found in the brain (11–13).

The TF gene exhibits a distinct pattern of tissue-specific expression *in vivo* and is inducible in a variety of cultured cell types. For example, it has been defined as an immediate-early gene in fibroblasts (11) and is induced in endothelial cells and cells of the monocyte lineage by inflammatory mediators (reviewed in reference 6). These data suggest that TF may participate in processes other than hemostasis.

All studies analyzing human TF antigen expression by immunohistochemistry have observed a diffuse staining throughout the brain parenchyma (9,10,14). Therefore, to date, it has not been possible to identify the cellular source of TF in the brain. In this study, we report the distribution of TF mRNA-positive cells in the murine CNS using *in situ* hybridization. Furthermore, we demonstrate that the signal for glial fibrillary acidic protein (GFAP), a marker for astrocytes in the CNS (reviewed in reference 15), colocalizes with the hybridization signal for TF mRNA in the parenchyma, indicating that the TF mRNA-positive cells are astrocytes. These results suggest that astrocytes, in addition to their roles in neuronal support and blood-brain barrier formation, may be intimately involved in preventing hemorrhage within the CNS. Finally, we observed increased TF mRNA expression in scrapie-infected murine brains in the presence of an extensive reactive astrocytosis.

Parts of this work were presented at the 22nd Annual Meeting of the Society for Neuroscience, Anaheim, CA, 25–30 October 1992; abstract number 540.10.

Address correspondence to N. Mackman, Department of Immunology, The Scripps Research Institute, 10666 North Torrey Pines Road, La Jolla, CA 92037.

Received for publication 15 December 1992 and in revised form 16 February 1993.

1. *Abbreviations used in this paper:* CNS, central nervous system; FCS, fetal calf serum; GFAP, glial fibrillary acidic protein; GAPDH, glyceraldehyde-3-phosphate dehydrogenase; TF, tissue factor.

J. Clin. Invest.

© The American Society for Clinical Investigation, Inc.

0021-9738/93/07/349/10 \$2.00

Volume 92, July 1993, 349–358

Methods

Animals. Adult, male SWR/j and C57BL/6j mice (breeding colony, The Scripps Research Institute) were used for all experiments. For infection with the Chandler strain of scrapie (16), 4–6-week-old mice were anesthetized with metaflane by inhalation and then injected intracerebrally with 30–50 μ l of a 10% scrapie-infected mouse brain homogenate. Scrapie-infected mice for in situ hybridization and immunohistochemistry were killed at 11 wk (preclinical), 16 wk (early clinical), and 21 wk (late clinical) after inoculation.

Tissue preparation. Mice were deeply anesthetized with 0.7g/kg body wt of chloral hydrate injected intraperitoneally, then transcardially perfused with 4% paraformaldehyde in chilled PBS. The brains were removed and postfixed in the same solution at 4°C overnight, before being dehydrated and embedded in paraffin. 3- μ m thick sections were cut using a rotary microtome, mounted onto "Superfrost plus" slides (Fisher Scientific Co., Pittsburgh, PA) and stored at room temperature before use.

Riboprobe preparation. The murine TF cDNA probe was an 821-bp fragment isolated from plasmid pcmTF2253 (17). This fragment was subcloned into the vectors pGEM-3Z and pGEM-4Z (Promega Corp., Madison, WI) and used as a template for the in vitro transcription of radiolabeled sense (pGEM-3Z) and antisense (pGEM-4Z) TF riboprobes using SP6 polymerase (Promega) in the presence of ³⁵S-UTP (> 1,200 Ci/mmol; Amersham Corp., Arlington Heights, IL). Templates were removed by digestion with RQ1 DNase (Promega) for 15 min at 37°C, and the riboprobes were purified by phenol/chloroform extraction and ethanol precipitation.

In situ hybridization. In situ hybridization was performed as previously described (18). Briefly, paraffin-embedded tissue sections were pretreated sequentially with xylene (3 \times 5 min), 2 \times SSC (300 mM NaCl, 30 mM sodium citrate, pH 7.0, containing 10 mM 2-mercaptoethanol, 1 mM EDTA) (1 \times 10 min), paraformaldehyde (1 \times 10 min, 4°C) and proteinase K (1 mg/ml in 500 mM NaCl, 10 mM Tris-HCl, pH 8.0) (1 \times 10 min). (Note: all incubations and washes were performed at 25°C unless specified otherwise.) Slides were prehybridized for 2 h in 100 μ l of prehybridization buffer (50% [wt/vol] formamide, 0.3 M NaCl, 20 mM Tris-HCl, pH 8.0, 5 mM EDTA, 0.02% polyvinylpyrrolidone, 0.02% Ficoll, 0.02% BSA, 10% [wt/vol] dextran sulphate, 10 mM dithiothreitol) at 42°C. Prehybridization buffer (20 μ l) (containing 2.5 mg/ml of tRNA and 600,000 cpm of the ³⁵S-labeled riboprobe) was then added, and the slides were hybridized for 18 h at 55°C. After hybridization, slides were treated with 2 \times SSC containing 10 mM 2-mercaptoethanol, 1 mM EDTA (2 \times 10 min), RNase A (20 mg/ml in 500 mM NaCl, 10mM Tris-HCl) (1 \times 30 min), 2 \times SSC (10 mM 2-mercaptoethanol, 1 mM EDTA) (2 \times 10 min), 0.1 \times SSC (10 mM 2-mercaptoethanol, 1 mM EDTA) (1 \times 2 h, 60°C) and 0.5 \times SSC (2 \times 10 min). Finally, after dehydration by immersion in a graded alcohol series containing 0.3 M NH₄Ac, the slides were dried, coated with NTB2 emulsion (Kodak; 1:2 in water), and exposed in the dark at 4°C for 8–12 wk. Slides were developed for 2 min in D19 developer (Kodak), fixed, washed in water (3 \times 5 min), and counterstained with hematoxylin and eosin. Serial sections were analyzed using a TF sense riboprobe as a control for nonspecific hybridization. No specific signal could be detected in these control hybridizations.

Immunohistochemistry. Sections were deparaffinized through a xylene and ethanol gradient, blocked in 5% normal calf serum in PBS for 30 min, then incubated overnight at 4°C in a humidity chamber with the primary antibody, rabbit anti-bovine GFAP (Dako Corp., Carpinteria, CA) diluted 1:400. Immunopositive cells were then visualized with the highly sensitive avidin biotin complex-horseradish peroxidase histochemistry procedure (Vector Laboratories, Burlingame, CA) according to the manufacturer's protocol, using a diaminobenzidine substrate (tetrahydrochloride salt; Sigma Immunochemicals, St. Louis, MO). For double labeling of the same tissue section, slides were initially subjected to in situ hybridization using a TF riboprobe. Slides were then removed from the 0.5 \times SSC wash before alcohol dehydra-

tion and treated for immunohistochemistry. After GFAP staining, the in situ hybridization protocol was continued with dehydration of the slides and coating with emulsion. Immunofluorescence was carried out basically as above except that the avidin biotin complex-horseradish peroxidase reagents were replaced with a goat anti-rabbit FITC-conjugated antibody (Caltag Laboratories Inc., San Francisco, CA), diluted 1:100. Controls were carried out in the absence of the primary antibody.

Tissue culture. Mouse primary astrocyte cultures were isolated from neonatal mice following the protocol of McCarthy and de Vellis (19). Briefly, neonatal mice were decapitated and the brains removed, leaving as much of the meninges behind as possible. The brains were disaggregated, first with a pipette, then with an 18' gauge needle and placed in poly-L-lysine-coated flasks. After 2 d the flasks were rapped to remove loosely adherent cells, and then on day 5 shaken overnight to remove oligodendrocytes and microglia. By immunofluorescence, such cultures in our laboratory are > 95% GFAP positive. The murine JCT cell line arose by spontaneous immortalization of an astrocyte in primary culture in our laboratory and expresses GFAP and S100 β protein by immunofluorescence, and glutamine synthetase mRNA by Northern blot, all markers of astrocytes (15) (de la Torre, J. C., and M. Eddleston, unpublished data). The human glioblastoma U373 MG and grade IV astrocytoma CCF-STTG1 cell lines were obtained from the American Type Culture Collection, Rockville, MD. The oligodendrocyte cell line 36C.21 was a gift from M. Carson and A. McMorris (Wistar, PA). The cell lines were kept at 37°C in DMEM-high glucose medium supplemented with 10% heat-inactivated FCS, penicillin, streptomycin, and 1% glutamine, except for U373 MG and PC12 cells, which had 1 mM sodium pyruvate or 5% horse serum added to the medium, respectively. The oligodendrocyte cell line 36C.21 was differentiated for 6 days in low serum (1% FCS) and 5 μ g/ml insulin. PC12 cells were differentiated to express a neuronal phenotype by treatment with 100 ng/ml β nerve growth factor for 72 hours (20).

Northern blot analysis. Mice were killed by cervical dislocation and then the organs quickly removed and snap frozen in liquid nitrogen. Total RNA was isolated from mouse brains by the guanidinium isothiocyanate-phenol chloroform method (21). PolyA⁺ RNA was then selected by a further cycle of oligo (dT)-cellulose (Invitrogen, San Diego, CA) chromatography. 4 μ g of polyA⁺ was size-fractionated on a 1% formaldehyde denaturing agarose gel, the RNA stained with ethidium bromide and the gel photographed. For tissue culture cells, total RNA was isolated and 10 μ g resolved on denaturing agarose gels as above. The RNA was transferred to nylon (Micron Separations Inc., Westboro, MA) using 20 \times SSC and the resultant blots ultraviolet cross-linked twice (Stratalinker; Stratagene Inc., La Jolla, CA) and prehybridized for 30 min in 2–3 ml of Quikhyb (Stratagene Inc.) at 55°C in a hybridization incubator (model 310; Robbins Scientific Corp., Sunnyvale, CA). Heat denatured DNA probe, labeled with [α -³²P]dCTP using random hexamers (Pharmacia LKB Biotechnology Inc., Piscataway, NJ), and salmon sperm DNA were added to the Quikhyb buffer to concentrations of 10 ng/ml, and 30 μ g/ml of buffer, respectively. Hybridization proceeded for 2.5 h at 55°C. Blots were washed twice at high stringency (0.2 \times SSC, 0.1% SDS, 60°C) for 15 minutes and then exposed to Kodak XAR-5 film with intensifying screens at -70°C. mRNA levels were quantitated by densitometric analysis of northern blot autoradiograms with a laser densitometer (Ultrascan XL; LKB, Bromma, Sweden). The 821-bp murine TF cDNA fragment described above, a 641-bp fragment of the human TF cDNA (22), or a rat GFAP cDNA fragment (gift of R. Milner, The Scripps Research Institute) were used to probe the blots. Variability in RNA loading was assessed using a cDNA encoding rat glyceraldehyde-3-phosphate dehydrogenase (23), a gift from L. Feng, The Scripps Research Institute.

Coagulation assay. Confluent monolayers of murine JCT and human U373 astrocyte cell lines were washed twice with Tris-buffered saline, scraped from the flask, divided into aliquots of 5 \times 10⁴ cells, and centrifuged at 1,500 g for 10 min at 4°C. The supernatant was removed and the pellets stored at -20°C. TF activity was assayed using a single-stage plasma coagulation assay as described (24). Cell lysates for coagu-

lation tests were prepared by resuspending the cell pellets in 100 μ l of 15 mM octyl β -D glucopyranoside, incubating for 15 min at 37°C, and then adding 200 μ l Hepes/saline (20 mM Hepes pH 6.0, 140 mM NaCl). The samples were vortexed and kept on ice before assaying. 100 μ l samples were added to 100 μ l prewarmed human citrated plasma in 15 \times 75-mm borosilicate glass tubes. After 30 s, 100 μ l of 20 mM CaCl₂ was added, the tubes rocked manually, and the time required for a visible fibrin gel to form noted. Functional TF was quantitated by using a standard curve established with phospholipid-reconstituted affinity-purified TF from human brain. For inhibition studies of human TF expressed by U373 cells, samples were incubated on ice for 25 min with three inhibitory monoclonal antibodies against human TF (TF8-5G9, TF9-9C3, and TF9-6B4) before the clotting assay. TF activity expressed by the JCT cells was compared to that expressed by BALB/c 3T3 fibroblast cells. The use of heterologous human plasma in these studies provides only a qualitative measurement of murine TF activity but does allow comparison of clotting activity between two murine cell lines.

Results

TF mRNA expression in the CNS. To determine the pattern of cell specific expression of TF, we performed in situ hybridization with a murine TF riboprobe on 3- μ m thick murine brain sections. The slides were counterstained with hematoxylin and eosin and examined by light microscopy.

There was striking expression of TF mRNA in the cells of the leptomeninges (Fig. 1 A). In areas where the arachnoid mater had been removed during tissue preparation, there was no signal associated with the remaining cells of the pia mater (data not shown), indicating that it was the arachnoid cells that expressed high levels of TF mRNA. As a control for specificity of the antisense TF riboprobe, serial sections were hybridized with a sense TF riboprobe but produced no specific signal (Fig. 1 B).

A regular scattering of strongly hybridizing cells was observed throughout the brain parenchyma, particularly within the gray matter (Fig. 1 C). Occasional TF mRNA-positive cells were also found within the white matter tracts, although the signal was less intense (Fig. 1 F). This pattern of TF mRNA expression was consistent with a neuroglial distribution. Furthermore, the hybridizing cells of both gray and white matter exhibited relatively large gray nuclei, no distinct nucleoli, uncondensed chromatin, and apparently sparse cytoplasm surrounding the nucleus, all morphological features typical of astrocytes.

In the cerebral cortex, TF mRNA-positive cells, similar to those shown in Fig. 1 C, occurred in all six layers (data not shown). Cells expressing TF mRNA were also observed scattered throughout the striatum, hypothalamus and thalamus, midbrain, pons, and medulla (data not shown). TF mRNA-positive cells were notably absent only from the molecular cell layer of the cerebellum, an area particularly rich in microglia (25). In the hippocampal formation, a less intense but specific hybridization signal was observed in cells present in Ammon's horn and the dentate gyrus (Fig. 1 D). In the olfactory lobe, TF mRNA-positive cells again occurred randomly but particularly within the external plexiform (Fig. 1 E) and internal granular layers. TF mRNA-positive cells exhibited a morphology and distribution consistent with that of astrocytes.

Cells cytologically identified as neurons were consistently negative for TF mRNA expression throughout the mouse brain using in situ hybridization (Fig. 1). For example, in the hippocampal formation the pyramidal cells of CA 1-3 (data not

shown), granular cells of the dentate gyrus (*dg*) and hilar neurons (*hn*) did not express detectable levels of TF mRNA (Fig. 1 D). In addition, Fig. 1 E shows that the mitral (*m*), tufted (*t*), periglomerular (*pg*), and internal granular (*g*) neurons of the olfactory lobe were all negative for TF mRNA expression, as were the Purkinje cells, granular cells, and neurons of the deep nuclei and molecular layer in the cerebellum (data not shown).

Oligodendrocytes, identified cytologically by their dark compact nuclei and arrangement in interfascicular rows (26), within the corpus callosum (Fig. 1 F), anterior commissure, cerebellar peduncles, and Vth cranial nerve tract of the medulla did not express detectable levels of TF mRNA.

The endothelial cells of parenchymal blood vessels were consistently negative (Fig. 1 G), as were cells aligned with the vessels. In addition, no expression was observed in cells of vessels present within either the sub-arachnoid space or the choroid plexus (Fig. 1 H). The ependymal cells lining the ventricles (Fig. 1 F), and the epithelial cells of the choroid plexus (Fig. 1 H) were negative. However, strongly positive cells were seen in the choroid plexus's core of connective tissue (Fig. 1 H); these cells had dark, compact nuclei suggestive of fibroblasts which are known to be present in the connective tissue stroma (27).

Astrocyte TF expression in vitro. Our studies described above suggested that astrocytes in vivo express relatively high levels of TF mRNA. To extend these observations, we analyzed TF expression in a variety of neural cells from three species. Initial northern blot analysis indicated that a mouse astrocyte cell line, termed JCT (Fig. 2), and mouse primary astrocyte cultures (data not shown) both constitutively expressed high levels of the 1.8-kb TF transcript. TF mRNA expression was then examined in human and rat astrocyte cell lines to determine if TF expression was a general feature of cultured astrocytes. Two human astrocyte cell lines (AST-U373 and AST-CCF) and one rat glioma cell line (AST-C6) also produced high levels of TF mRNA (Fig. 2), indicating that cultured astrocytes of three species constitutively expressed TF mRNA.

In addition to these studies on astrocytes, we assessed the level of TF mRNA expression in other cultured CNS cell types. GT1-7 cells, a murine hypothalamic neuronal cell line (28), expressed TF mRNA, although the level was significantly lower than that of JCT astrocytes. The rat oligodendrocyte cell line, 36C.21, expressed TF mRNA, but again at levels lower than the rat C6 astrocytes. Lastly, the pheochromocytoma cell line, PC12, both undifferentiated and differentiated with β NGF to produce a neuronal phenotype (20), failed to express detectable levels of TF mRNA. Total RNA from both murine brain and kidney were used as positive controls because these tissues express high levels of the 1.8-kb TF mRNA (29). Murine B cells were used as a negative control and, as expected, did not express the TF transcript.

After our observations that cultured astrocytes express TF mRNA, we sought to determine whether astrocytes produced a functional procoagulant protein. Because it is not possible to identify the cellular source of functional protein in whole brain extracts, the total cellular TF protein levels of murine JCT and human U373 astrocyte cells were analyzed using a single-stage clotting assay. JCT cells constitutively expressed high levels of procoagulant activity ($2.3 \pm 0.3 \times 10^3$ mU/ 10^6 cells, mean \pm SD, $n = 7$), comparable to the level expressed by a murine fibroblast cell line, BALB/c 3T3 cells ($1.2 \pm 0.2 \times 10^3$ mU/ 10^6 cells, $n = 5$). U373 cells also expressed high levels of

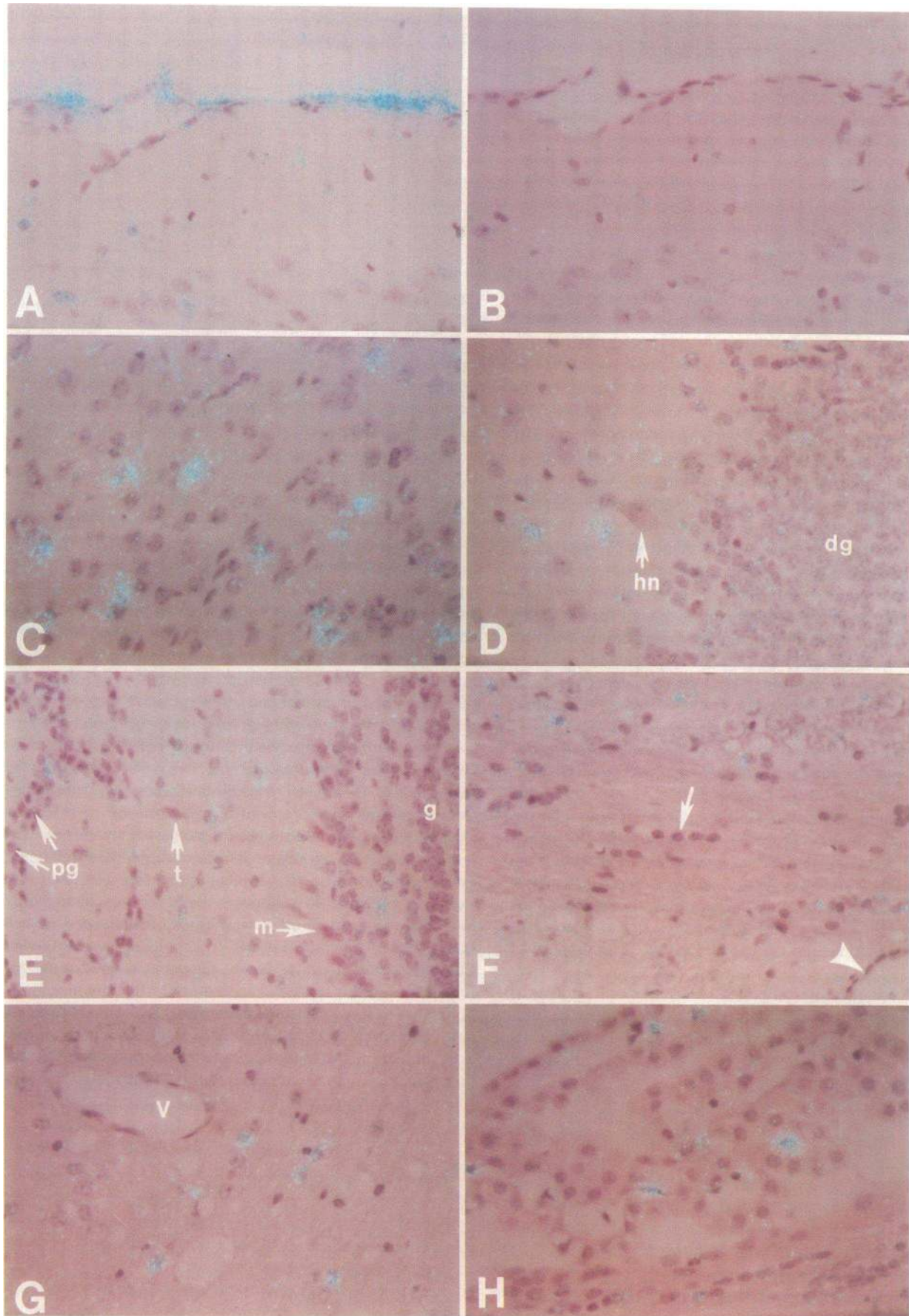


Figure 1. Tissue factor mRNA expression in the CNS. Normal mouse brain sections were hybridized to ^{35}S -labeled sense (B) or antisense (A, C-H) cRNA probes for murine TF. Sections were subsequently dipped in NTB-2 photographic emulsion, exposed for 11 wk at 4°C , developed

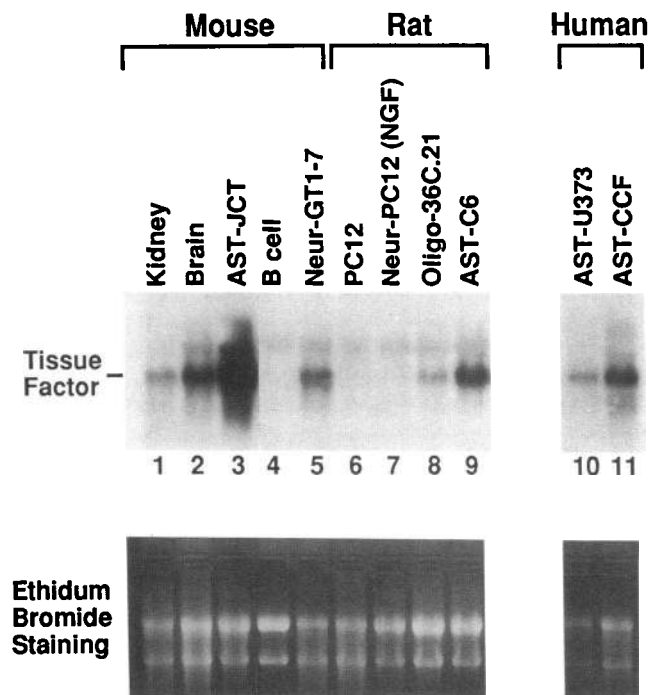


Figure 2. TF is expressed in astrocyte cell lines of various species. Total RNA was isolated from mouse kidney and brain, the murine astrocyte cell line JCT, the rat glioma cell line C6, two human astrocytic cell lines U373 MG and CCF-STTG1, the rat oligodendrocyte cell line 36C.21, the mouse neuronal cell line GT1-7, rat PC12 cells both undifferentiated, and differentiated with bNGF, and as a negative control the BALB/c mouse myeloma B cell line J558L. 10 μ g of each RNA was resolved on a formaldehyde denaturing gel, transferred to a nylon membrane, and hybridized sequentially to 32 P-labeled murine and human TF cDNA probes. This was required because under the stringent conditions used the mouse TF probe did not cross-hybridize with the human TF mRNA. The membrane was washed at high stringency (0.2 \times SSC, 60 $^{\circ}$ C) and exposed overnight to autoradiography. Various housekeeping genes used (GAPDH, CHO-B, and β -actin) all varied in their expression between the different cell lines and species. Therefore, the original ethidium bromide staining of the gel was used to indicate RNA loading.

procoagulant activity ($2.2 \pm 0.4 \times 10^3$ mU/ 10^6 cells, $n = 4$) which could be attributed to TF since it was inhibited by > 99% with monoclonal antibodies to human TF (30).

In conclusion, astrocytes in vitro expressed high levels of TF mRNA and functional procoagulant protein. In addition,

other cultured neural cell types were able to express TF mRNA but always at levels significantly lower than those expressed by astrocyte cell lines.

Modulation of TF mRNA expression in vivo. The final series of experiments examined whether TF mRNA expression was regulated in the brain in vivo in response to a specific neurological insult. We analyzed the brains of mice infected with the slow virus scrapie for two reasons. Firstly, there is an extensive activation of astrocytes in the disease (31), during which astrocytes undergo a phenotypic change, expressing greater levels of many molecules including GFAP (32). Importantly, in all neurological conditions studied thus far, phenotypic change of astrocytes in situ rather than migration or proliferation accounts for the majority of new GFAP-expressing astrocytes seen after insult (reviewed in reference 33). Secondly, the disease lacks both mononuclear cell infiltration and breakdown of the blood-brain barrier (reviewed in reference 31), and therefore any modulation of TF expression would occur independently of mononuclear cells and plasma proteins.

Serial 3- μ m thick sections of control or scrapie-infected brain were either stained by immunohistochemistry for GFAP or hybridized with an antisense TF riboprobe. Scrapie-infected brains contained many more hypertrophic, strongly stained astrocytes than control brains (Fig. 3), reflecting the extensive astrocytosis following infection. Nevertheless, we found no evidence for increased numbers of astrocytes in infected brains. GFAP-expressing astrocytes from both control and infected brains were TF mRNA-positive on serial sections (Fig. 3); however, some TF mRNA-positive cells were observed in both control and infected brains that did not stain for GFAP. Double-labeling on serial sections has limitations because cells on one section may not be present on the next section. In addition, the observed GFAP-negative, TF mRNA-positive cells may be astrocytes that are expressing GFAP below the detection threshold of the immunohistochemistry technique. This explanation is more likely in control brains which do not exhibit astrocytosis. The glia limitans, which forms the boundary between brain and meninges, stained strongly with GFAP but exhibited no hybridization to the antisense TF riboprobe because it contains few astrocyte cell bodies (Fig. 3, A and B).

The hybridization signal associated with cells in scrapie-infected brain sections appeared to be consistently more intense than the signal associated with astrocytes in uninfected brain sections present on the same slide. The signal was quantitated by counting grains over individual cells: control brains, mean number of grains/cell = 15.3, SD = 4.5, $n = 100$; scrapie-infected brains, mean = 32 grains/cell, SD = 7.8, $n = 86$. These

in D19, and counterstained with hematoxylin and eosin. All views used polarized light epiluminescence and are at a magnification of 400 unless otherwise stated; positive hybridization signals appear as blue-green grains. (A) and (B) Leptomeninges hybridized with antisense and sense TF riboprobes, respectively, using serial sections. Cells of the leptomeninges hybridized very strongly to the antisense probe, while the sense riboprobe produced no specific signal. (C) Scattered TF mRNA-positive cells in the deep nuclei of the cerebellum. Using bright field microscopy, these cells exhibited large, pale gray nuclei consistent with the cells being astrocytes. Neuronal cells did not hybridize to the probe. (D) The junction of the hilus and granular cell layers of the hippocampal dentate gyrus. TF mRNA-positive cells occurred randomly throughout the hippocampal formation but with a lower signal in the dense neuronal layers; neither the dentate granular (*dg*) nor hilar (*hn*) neurons exhibited a positive signal. (E) Cross-section ($\times 200$) of olfactory lobe showing the mitral neurons (*m*), the periglomerular neurons (*pg*), the tufted cells (*t*), and the neurons of the granular layer (*g*). None of these specialized neurons exhibited a positive signal but were instead surrounded by scattered positive glia. (F) The corpus callosum showing interfascicular rows of nonhybridizing oligodendrocytes (*arrow*) with the occasional weakly positive fibrous astrocyte. Ependymal cells (*arrowhead*) lining the lateral ventricle were also negative. (G) A blood vessel (*v*) within the neural parenchyma, demonstrating that cells of the vessel wall did not hybridize to the TF probe. Positive parenchymal cells can be seen in the same section. (H) The epithelial cells of the choroid plexus did not express TF. However, occasional positive cells did occur in the connective tissue stroma of the vascularized core. These cells were not associated with the blood vessels and may be collagen-secreting fibroblasts.

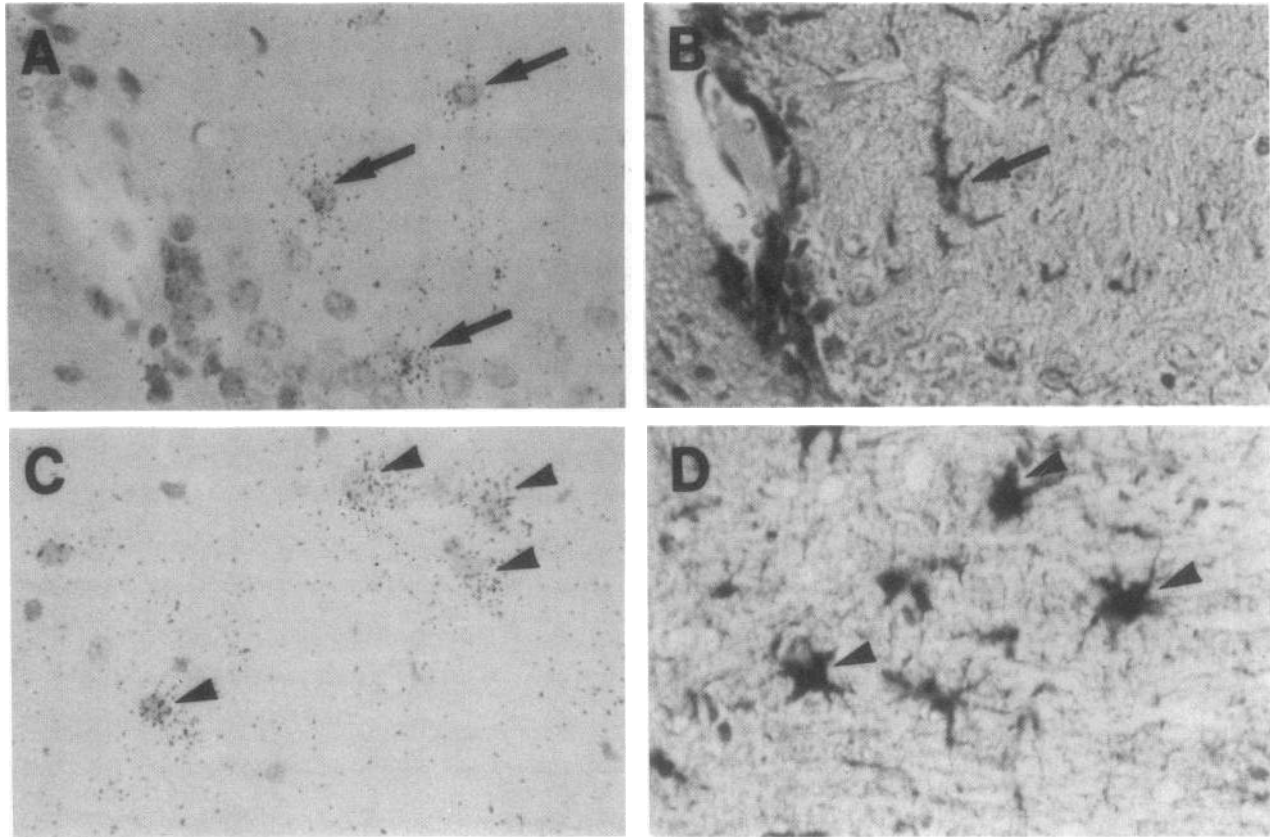


Figure 3. TF mRNA expression in control and scrapie-infected brains. Serial 3- μ m thick normal (*A, B*) or scrapie-infected (*C, D*) mouse brain hippocampal sections were analyzed for TF mRNA or GFAP expression. Panels *A* and *C* were hybridized with 35 S-labeled antisense mouse TF riboprobe and viewed under bright field to reveal the hybridization signal as black grains. Panels *B* and *D* were reacted with polyclonal anti-GFAP antibodies to identify the starlike cell bodies of the astrocytes. Computer-assisted electronic mapping, in which photographic images were taken of serial sections, labeled cells marked and then the images overlaid on the computer monitor, was used to align sections. In the uninfected brain, one of the three TF mRNA-positive cells (*A*) expressed GFAP (*B*). Three of the four TF mRNA-positive cells in the scrapie-infected brain (*C*) expressed GFAP (*D*). The glia limitans lining the brain contained high levels of GFAP (*B*) but did not hybridize to the TF riboprobe.

data revealed an increase in TF mRNA-expression in astrocytes after infection. Similar results were observed in three independent experiments. TF mRNA expressing cells were also more prevalent in the white matter tracts in scrapie-infected brains (data not shown). These results suggested that TF mRNA expression in astrocytes may be upregulated during scrapie infection.

Due to the inherent problems associated with using serial sections to identify the TF mRNA-positive cell population, *in situ* hybridization for TF and immunohistochemistry for GFAP were performed on the same sections of scrapie-infected mouse brain. The great majority of GFAP-positive cells expressed high levels of TF mRNA (Fig. 4, *A-D*), and no specific hybridization signal was associated with nonastrocytes in the parenchyma. Thus, within the detection limits of the *in situ* hybridization assay, astrocytes were the only cell type to express TF mRNA within the parenchyma of scrapie-infected brains. Strongly TF mRNA-expressing cells of the arachnoid mater were clearly identified (Fig. 4, *E* and *F*) whereas cells directly in contact with the glia limitans were negative.

To quantitate more accurately this apparent increase in TF mRNA expression during reactive astrocytosis, TF mRNA levels were compared by Northern blot analysis using RNA derived from scrapie-infected and uninfected mouse brains. PolyA⁺ RNA was isolated from the brains of either scrapie-in-

fecting mice exhibiting clinical symptoms of gait disturbances, kyphosis, and somnolence (34), or uninfected age-matched control mice. The RNA was resolved by gel electrophoresis and the resulting Northern blots hybridized with a GFAP cDNA probe to assess the astrocytosis in the diseased brains. GFAP mRNA levels, indicative of an activation of astrocytes, were markedly increased in infected brains (Fig. 5). The blots were subsequently hybridized with a murine TF cDNA fragment which revealed that the level of TF mRNA was increased in scrapie-infected brains compared to uninfected controls (Fig. 5). The TF mRNA signal was quantitated by densitometry scanning and normalized using glyceraldehyde-3-phosphate dehydrogenase to control for RNA loading. Comparison of six control brains and six scrapie-infected brains in two independent experiments indicated that TF mRNA levels were increased 3.2-fold (SD = 1.45) in infected brains. Using the Student's *t* test, this increase is statistically significant ($0.01 > P > 0.001$). Thus, TF mRNA levels in the brain can be modulated *in vivo* by scrapie infection.

Discussion

In this study, the colocalization of murine TF mRNA expression and GFAP indicated that TF biosynthesis in the neural

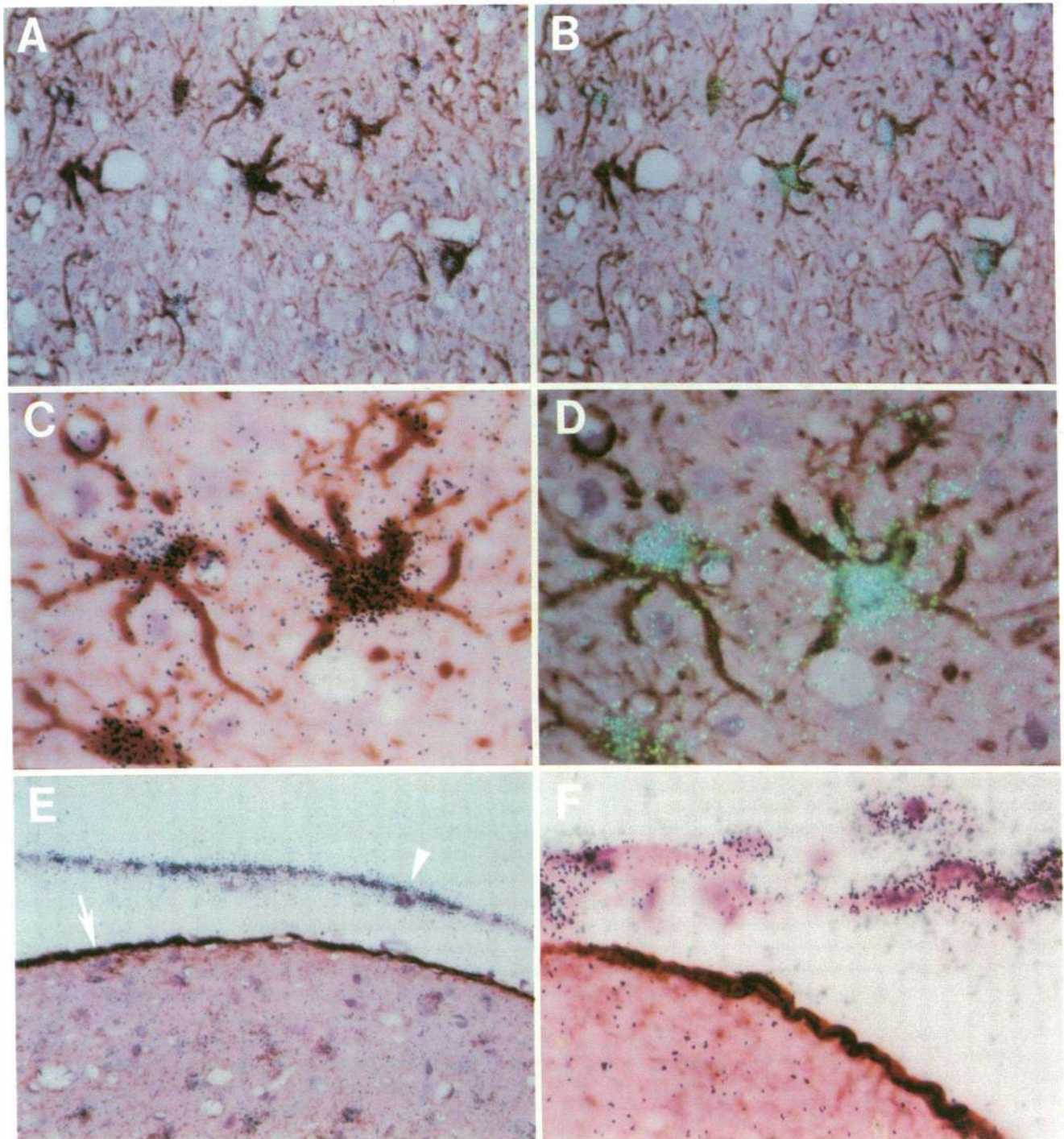


Figure 4. TF mRNA is expressed in astrocytes in the scrapie-infected CNS. 3- μ m thick scrapie-infected mouse brain sections were sequentially hybridized with a 35 S-labeled antisense mouse TF riboprobes and then reacted with polyclonal anti-GFAP antibodies to identify astrocytes. TF mRNA-positive cells expressed GFAP (A–D) indicating that they were astrocytes. The GFAP-positive glia limitans lining the brain (arrow, E, F) is negative for TF mRNA expression because of the lack of astrocyte cell bodies in this limiting boundary. In contrast, the overlying arachnoid mater (arrowhead, E, F) is strongly positive. Positive hybridization signals appear as black grains (A, C, E, F) or as blue-green grains using polarized light epiluminescence (B, D). The brown precipitate identifies astrocyte cell bodies and structures containing GFAP. Magnification is either $\times 400$ (A, B, E) or $\times 1,000$ (C, D, F).

parenchyma was predominantly a function of astrocytes. High level expression of TF mRNA in primary mouse astrocyte cultures and four astrocyte cell lines from mouse, rat, and human supported the hypothesis that astrocytes are the major source

of TF in the mouse brain. Further in vitro analysis demonstrated that astrocyte-derived TF protein had functional procoagulant activity. These results were consistent with a recent study demonstrating that Bergmann glia, a specialized form of

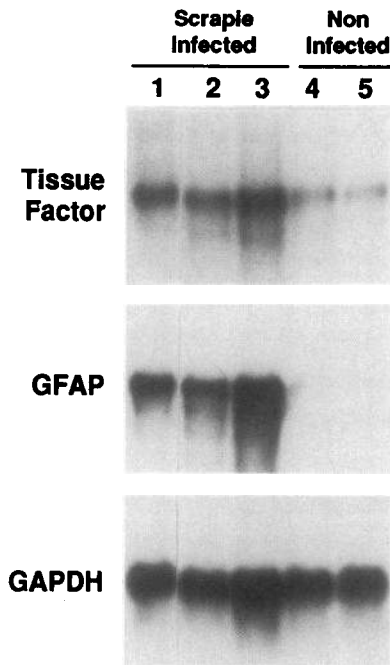


Figure 5. Tissue factor mRNA is increased in the CNS during scrapie-induced astrocytosis. 4–6 wk-old mice were intracerebrally inoculated with a 10% scrapie-infected brain homogenate. During the late clinical stages (18–20 wk after inoculation), these mice and uninfected controls were killed and polyA⁺ RNA isolated from each brain. The RNA was resolved on a denaturing gel, blotted, and initially hybridized with a GFAP cDNA fragment to analyze the level of astrocytosis. Subsequently, the blot was hybridized with a murine TF cDNA fragment. Finally, RNA

loading in each lane was determined by hybridization with the housekeeping gene GAPDH. Scrapie-infected brains exhibiting astrocytosis shared a dramatic increase in GFAP expression and densitometric scanning of the autoradiograms, normalized to levels of GAPDH, revealed a 3.2 fold increase in TF mRNA levels. Data from one of two independent experiments are shown.

astrocyte in the cerebellum, express high levels of TF mRNA in the murine brain (29).

Arachnoid meningeal cells surrounding the brain expressed high levels of TF mRNA while identifiable neurons and nonastrocyte glial cells did not express TF mRNA in the parenchyma at levels detectable by *in situ* hybridization (Figs. 1 and 4). We found no evidence for TF mRNA expression by microglia. The lack of detectable TF mRNA in specific neuronal cell populations correlated with the absence of human TF antigen in Purkinje and granular neurons by immunohistochemistry (10). However, previous studies using anti-human TF antibodies have reported a diffuse TF antigen expression throughout the parenchyma (9, 10, 14). This may suggest that nonastrocyte cells of the brain also express TF but at levels below the detection threshold of *in situ* hybridization. This hypothesis is consistent with the low level of TF mRNA expression we observed in nonastrocyte cell lines *in vitro* (Fig. 2).

TF expression in astrocyte endfeet (see Fig. 6 below) may explain the earlier reported strong expression of TF antigen surrounding major (14) and micro (35) CNS vessels and deep to the pia mater in the parenchyma (9). In addition, TF mRNA expression by cells of the arachnoid mater is consistent with previous immunohistochemical localization of TF in the leptomeninges of human brain (10). In contrast, the cells of the pia mater, which form the adventitia of large blood vessels in the CNS (36), did not express detectable levels of TF mRNA. TF expression by fibroblast-like cells in the stroma of the choroid plexus has been observed using anti-human TF monoclonal antibodies (T. Drake, personal communication), consistent with our data. The greater expression of TF mRNA

by cells in the gray matter relative to white matter observed in our study agrees with the reported distribution of neural TF protein by immunohistochemistry, ELISA, and functional assays (9, 10, 35).

Astrocytes constitute a substantial proportion of the CNS, participating in a number of important physiological processes. In the developing brain, cells of the astrocyte lineage are believed to form a scaffold along which neurons migrate to find their position in the neural cytostructure. In the adult brain, astrocytes buffer neurons from changes in ion and toxic neurotransmitter concentrations, supply trophic support to neurons and other neural cells (reviewed in references 37–39), and may play an important role in signaling (reviewed in reference 38). Roles for astrocytes in the induction of the blood-brain barrier (40) and control of the microvascular blood flow in the brain (38) have also been proposed. Here, we provide new evidence that astrocytes also function in the control of hemostasis at the blood/CNS interface by expressing tissue factor.

The observed distribution of TF expression in astrocytes and arachnoid meningeal cells is consistent with a primary role for TF in CNS hemostasis. The meninges cover the surface of the brain, separating the brain parenchyma from peripheral tissues. The basement membrane of the innermost pia mater layer of the meninges lies directly in contact with the glia limitans, a boundary formed by astrocyte endfeet (Fig. 6, A, B, and D). These endfeet are extensions of the termini of astrocyte processes extending from the cell bodies which may lie at some distance in the parenchyma (Fig. 6 B). As blood vessels pass from the subarachnoid space into the neural parenchyma, they are ensheathed within the glia limitans, which continues to surround every blood vessel within the brain (Fig. 6, C and E), from arteries through capillaries to veins (see reference 36 for a detailed description). Expression of TF in arachnoid meningeal cells and astrocyte endfeet processes would result in the complete ensheathment of the interface between the CNS and cerebrospinal fluid/blood by cells that express TF, thus forming a “hemostatic envelope” around the CNS. In the periphery, in contrast, TF expression is predominantly restricted to the tunica adventitia of the major vessels and myoepithelial sheathes surrounding each organ (9, 10).

The extensive expression of TF may reflect the sensitivity of the brain to hemorrhage and the potential consequences to the organism of dysregulated neuronal function. Studies have suggested that neuronal dysfunction and seizure activity after hemorrhagic injury is related to the induction of free radicals by iron moieties released from extravasated blood, and the subsequent peroxidation of lipids (reviewed in references 41, 42). A high level of TF expression around the neural blood vessels might also have damaging consequences for the organism during disease or injury. In particular, exposure of high levels of TF protein from the CNS after damage to neural blood vessels could account for the transient disseminated intravascular coagulation seen following acute, severe brain trauma (43, 44).

In addition to its role in hemostasis, TF may function in other processes within the CNS. In this study, we found that TF mRNA levels were increased 3.2-fold in scrapie-infected mouse brains in the presence of an extensive reactive astrocytosis. It is of note that astrocytes were the only cell type observed to express TF mRNA in double labeling experiments of scrapie-infected brains. We speculate that increased TF expression in astrocytes may account, in part, for the increase in total brain TF mRNA after infection, although an increase in TF

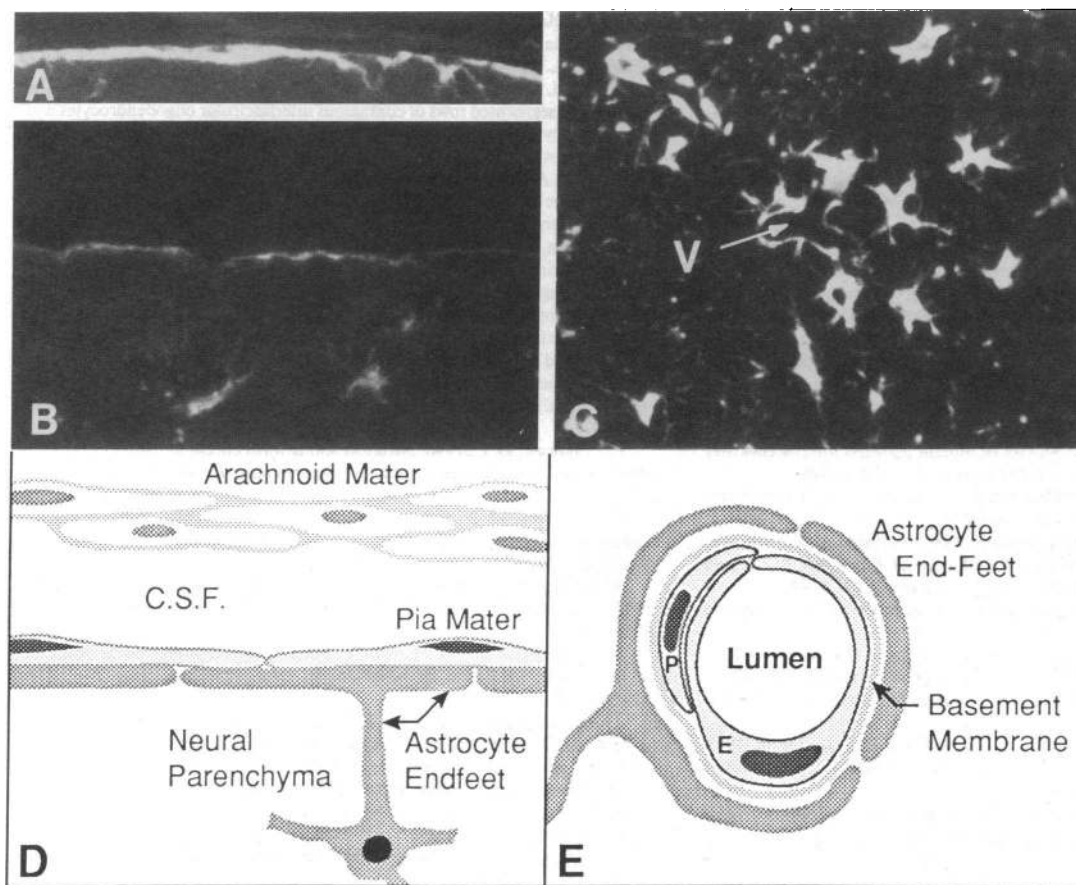


Figure 6. The relationship of astrocytes to the glia limitans. Astrocyte processes extending away from the cell body terminate to form endfeet which wrap around the neural vasculature and line the neural parenchyma/meninges boundary, forming the glia limitans. (A, B, C) Astrocyte endfeet processes lining the neural/meningeal interface, forming the glia limitans externa (A, B), and ensheathing a neural blood vessel (v), forming the glia limitans interna (C), were identified with immunofluorescence using anti-GFAP antibodies on sections of mouse brain. Processes can be seen extending towards the glia limitans from the astrocyte cell bodies which frequently lie at some distance (B). (D, E) Schematic representations to illustrate the relationship of astrocyte

cell bodies and endfeet processes to the glia limitans and other cell types at the interface of the brain with nonneural tissue and around blood vessels. (D) The leptomeninges are made up of arachnoid and pia maters and the interlying subarachnoid space which is filled with cerebrospinal fluid (CSF). This structure encloses the brain and via the pia mater is in intimate contact with the astrocyte glia limitans. Blood vessels are located within the arachnoid layer and must traverse the subarachnoid space before entering the brain parenchyma ensheathed in a layer of pia mater and glia limitans. (E) In the neural parenchyma, vascular endothelial cells (E) and pericytes (p) are enclosed within a basement membrane, which is itself ensheathed by the astrocyte endfeet of the glia limitans interna.

expression below the detectable threshold of in situ hybridization in cell types other than astrocytes cannot be discounted. The absence of vascular damage during scrapie infection supports the possibility that TF is fulfilling functions in the CNS other than the control of hemorrhage during the reactive astrocyte response. Consistent with other roles for this transmembrane receptor in neurobiology, TF is highly expressed in peripheral nerves (10) and in the supporting cells of autonomic ganglia (9, 10). TF may be involved in the interaction between neurons and their supporting cells, either directly through binding to another receptor, or indirectly through the generation of proteases such as thrombin (7). The recent evidence that coagulation proteases may be involved in the pathogenesis of human diseases such as Alzheimer's disease (reviewed in reference 45), suggests that it will be important to understand the roles of TF in the CNS.

Acknowledgments

The technical assistance of T. Thinnes and B. Fowler is gratefully acknowledged. We thank L. Feng for the GAPDH cDNA, R. Milner for the GFAP cDNA fragment, M. Carson and A. McMorris for the 36C.21 cells, and N. Gascoigne for the J558L myeloma cell line RNA;

F. Bloom and W. Young for help with the computer-assisted electronic mapping; and F. Bloom, N. Bang, R. Boyajian, and L. Mucke for critical review of the manuscript.

This research was supported by U.S. Public Health grants P50-MHA47680 (M. Eddleston, N. Mackman, J. de la Torre, T. Edgington, M. Oldstone); the U.S. Army Medical Research and Development Command under contract No. DAMD 17-90-C-0070 (M. Eddleston, J. de la Torre, M. Oldstone); National Institutes of Health grant HL-48872 (N. Mackman); and National Institutes of Health grant HL-47819 (D. J. Loskutoff).

References

1. National Center for Health Statistics. 1992. Advance report of final mortality statistics, 1989. *Monthly Vital Statistics Report*. Vol. 40, No. 8, Suppl. 2. Public Health Service, Hyattsville, MD.
2. Mackay, A., and B. C. Nias. 1979. Strokes in the young and middle-aged: consequences to the family and to society. *J. R. Coll. Physicians (Lond.)*. 13:106-112.
3. del Zoppo, G. J., M. S. Pessin, E. Mori, and W. Hacke. 1991. Thrombolytic intervention in acute thrombotic and embolic stroke. *Semin. Neurol.* 11:368-384.
4. Bach, R. R. 1988. Initiation of coagulation by tissue factor. *CRC Crit. Rev. Biochem.* 23:339-368.
5. Edgington, T. S., N. Mackman, K. Brand, and W. Ruf. 1991. The structural biology of expression and function of tissue factor. *Thromb. Haemostasis*. 66:67-79.

6. Edgington, T. S., N. Mackman, S. T. Fan, and W. Ruf. 1992. Cellular immune and cytokine pathways resulting in tissue factor expression and relevance to septic shock. *Nouv. Rev. Fr. Hematol.* 34(Suppl.):S15-S27.
7. Coughlin, S. R., T.-K. H. Vu, D. T. Hung, and V. I. Wheaton. 1992. Expression cloning and characterization of a functional thrombin receptor reveals a novel proteolytic mechanism of receptor activation. *Semin. Thromb. Hemost.* 18:161-166.
8. Bazan, J. F. 1990. Structural design and molecular evolution of a cytokine receptor superfamily. *Proc. Natl. Acad. Sci. USA.* 87:6934-6938.
9. Drake, T. A., J. H. Morrissey, and T. S. Edgington. 1989. Selective cellular expression of tissue factor in human tissues. *Am. J. Pathol.* 134:1087-1097.
10. Fleck, R. A., L. V. M. Rao, S. I. Rapaport, and N. Varki. 1990. Localisation of human tissue factor antigen by immunostaining with monospecific, polyclonal anti-human tissue factor antibody. *Thromb. Res.* 57:765-781.
11. Hartzell, S., K. Ryder, A. Lanahan, L. F. Lau, and D. Nathans. 1989. A growth factor-responsive gene of murine BALB/c 3T3 cells encodes a protein homologous to human tissue factor. *Mol. Cell. Biol.* 9:2567-2573.
12. Astrup, T. 1965. Assay and content of tissue thromboplastin in different organs. *Thromb. Diath. Haemorrh.* 14:401-416.
13. Williams, W. J. 1966. The activity of human placenta microsomes and brain particles in blood coagulation. *J. Biol. Chem.* 241:1840-1846.
14. McComb, R. D., K. A. Miller, and S. D. Carson. 1991. Tissue factor antigen in senile plaques of Alzheimer's disease. *Am. J. Pathol.* 139:491-494.
15. Dahl, D., H. Björklund, and A. Bignami. 1986. Immunological markers in astrocytes. In *Astrocytes. Cell Biology and Pathology of Astrocytes*. S. Fedoroff and A. Vernadakis, editors. Academic Press, Inc., Orlando, FL. 1-25.
16. Chandler, R. L. 1961. Encephalopathy in mice produced by inoculation with scrapie brain material. *Lancet.* i:1378-1379.
17. Mackman, N., S. Imes, W. H. Maske, B. Taylor, A. J. Lusic, and T. A. Drake. 1992. Structure of the murine tissue factor gene. Chromosome location and conservation of regulatory elements in the promoter. *Arterioscler. Thromb.* 12:474-483.
18. Keeton, M., Y. Eguchi, M. Sawdey, C. Ahn, and D. J. Loskutoff. 1993. Cellular localisation of type I plasminogen activator inhibitor mRNA and protein in murine renal tissue. *Am. J. Pathol.* 142:59-70.
19. McCarthy, K. D., and J. de Vellis. 1980. Preparation of separate astroglial and oligodendroglial cell cultures from rat cerebral tissue. *J. Cell Biol.* 85:890-902.
20. Greene, L. A., and A. S. Tischler. 1976. Establishment of a noradrenergic clonal line of rat adrenal pheochromocytoma cells which respond to nerve growth factor. *Proc. Natl. Acad. Sci. USA.* 73:2424-2428.
21. Chomczynski, P., and N. Sacchi. 1987. Single-step method of RNA isolation by acid guanidinium thiocyanate-phenol-chloroform extraction. *Anal. Biochem.* 162:156-159.
22. Morrissey, J. H., H. Fakhrai, and T. S. Edgington. 1987. Molecular cloning of the cDNA for tissue factor, the cellular receptor for the initiation of the coagulation protease cascade. *Cell.* 50:129-135.
23. Tso, J. Y., X.-H. Sun, T.-H. Kao, K. S. Reece, and R. Wu. 1985. Isolation and characterization of rat and human glyceraldehyde-3-phosphate dehydrogenase cDNAs: genomic complexity and molecular evolution of the gene. *Nucleic Acids Res.* 13:2485-2502.
24. Gregory, S. A., R. S. Kornbluth, H. Helin, H. G. Remold, and T. S. Edgington. 1986. Monocyte procoagulant inducing factor: a lymphokine involved in the T cell-instructed monocyte procoagulant response to antigen. *J. Immunol.* 137:3231-3239.
25. Polak, M., F. D'Amelio, J. E. Johnson, and W. Haymaker. 1982. Microglial cells: origins and reactions. In *Histology and Histopathology of the Nervous System*. W. Haymaker and R. D. Adams, editors. Charles C. Thomas Publisher, Springfield, IL. 481-559.
26. Suzuki, M., and G. Raisman. 1992. The glial framework of central white matter tracts: segmented rows of contiguous interfascicular oligodendrocytes and solitary astrocytes give rise to a continuous meshwork of transverse and longitudinal processes in the adult rat fimbria. *Glia.* 6:222-235.
27. Peters, A., S. L. Palay, and H. deF. Webster. 1991. Choroid plexus. In *The Fine Structure of the Nervous System. Neurons and Their Supporting Cells*. Oxford University Press, New York. 328-343.
28. Mellon, P. L., J. J. Windle, P. C. Goldsmith, C. A. Padula, J. L. Roberts, and R. I. Weiner. 1990. Immortalization of hypothalamic GnRH neurons by genetically targeted tumorigenesis. *Neuron.* 5:1-10.
29. Mackman, N., M. B. Sawdey, M. R. Keaton, and D. J. Loskutoff. 1992. Murine tissue factor gene expression by lipopolysaccharide in vivo: tissue and cell specificity and regulation by lipopolysaccharide. *Am. J. Pathol.* 143:1-8.
30. Morrissey, J. H., D. S. Fair, and T. S. Edgington. 1988. Monoclonal antibody analysis of purified and cell-associated tissue factor. *Thromb. Res.* 52:247-261.
31. Gajdusek, D. C. 1990. Subacute spongiform encephalopathies: transmissible cerebral amyloidoses caused by unconventional "viruses." In *Virology*. B. N. Fields and D. M. Knipe, editors. Raven Press Ltd., New York. 2289-2324.
32. Eddleston, M. P., and L. Mucke. 1993. The molecular profile of reactive astrocytes—implications for their role in neurologic disease. *Neuroscience.* 54:15-36.
33. Norton, W. T., D. A. Aquino, I. Hozumi, F.-C. Chiu, and C. F. Brosnan. 1992. Quantitative aspects of reactive gliosis: a review. *Neurochem. Res.* 17:877-885.
34. Eklund, C. M., W. J. Hadlow, and R. C. Kennedy. 1963. Some properties of the scrapie agent and its behaviour in mice. *Proc. Soc. Exp. Biol. Med.* 112:974-979.
35. del Zoppo, G. J., J.-Q. Yu, B. R. Copeland, W. S. Thomas, J. Schneiderman, and J. H. Morrissey. 1992. Tissue factor localisation in non-human primate cerebral tissue. *Thromb. Haemostasis.* 68:642-647.
36. Peters, A., S. L. Palay, and H. deF. Webster. 1991. Blood vessels. In *The Fine Structure of the Nervous System. Neurons and Their Supporting Cells*. Oxford University Press, New York. 344-355.
37. Fedoroff, S., and A. Vernadakis. 1986. *Astrocytes*. Vol. 1, 2, and 3. Academic Press, Orlando, FL.
38. Barres, B. A. 1991. New roles for glia. *J. Neurosci.* 11:3685-3694.
39. Bevan, S. 1990. Ion channels and neurotransmitter receptors in glia. *Semin. Neurosci.* 2:467-481.
40. Janzer, R. C., and M. C. Raff. 1987. Astrocytes induce blood-brain barrier properties in endothelial cells. *Nature (Lond.)* 325:253-257.
41. Halliwell, B., and J. M. C. Gutteridge. 1985. Lipid peroxidation: a radical chain reaction. In *Free Radicals in Biology and Medicine*. Clarendon Press, Oxford. 139-189.
42. Willmore, L. J., and W. J. Triggs. 1991. Iron-induced lipid peroxidation and brain injury responses. *Int. J. Dev. Neurosci.* 9:175-180.
43. Keimourtz, R. M., and B. L. Annis. 1973. Disseminated intravascular coagulation associated with massive brain injury. *J. Neurosurg.* 39:178-180.
44. Noormaa, U., and A. Tikki. 1979. Cerebrovascular intravascular coagulation and increased platelet coagulation as mechanisms of cerebral ischemia in patients with acute cerebrovascular diseases and brain injury. *Acta Neurol. Scand.* 60(Suppl. 72):630-631.
45. Marx, J. 1992. A new link in the brain's defences. [News]. *Science (Wash. DC)* 256:1278-1280.